This document is a preprint of: M. Sigmund, R. Bomfin, M. Chafii et al., "Waveform Design for Power-Domain Asynchronous NOMA," in Proceedings of IEEE Vehicular Technology Conference (VTC Spring 2022), Helsinki, Finland, Jun 2022.

Waveform Design for Power-Domain Asynchronous NOMA

Martin Sigmund *, Roberto Bomfin *, Marwa Chafii†‡, Ahmad Nimr *, Gerhard Fettweis *
*Vodafone Chair Mobile Communication Systems, Technische Universität Dresden, Dresden, Germany
{martin.sigmund,roberto.bomfin,ahmad.nimr,gerhard.fettweis}@tu-dresden.de
† Engineering Division, New York University (NYU) Abu Dhabi, Abu Dhabi, UAE
‡ NYU WIRELESS, NYU Tandon School of Engineering, New York, USA
marwa.chafii@nyu.edu

***Abstract*—Power-domain asynchronous non-orthogonal multiple access (ANOMA) is a novel radio access technique with non-orthogonal resource allocation that enables asynchronous transmissions and has an enhanced spectrum efficiency compared to orthogonal multiple access. In this work, an iterative receiver is derived for linearly modulated waveforms. Orthogonal frequency division multiplexing (OFDM), single-carrier (SC) and orthogonal chirp division multiplexing (OCDM) are investigated. The receiver is based on triangular successive interference cancellation (T-SIC) in combination with a minimum mean square error parallel interference cancellation (MMSE-PIC) detector. It is advantageous to utilize a waveform which spreads the data symbols in the frequency domain as OCDM or SC in order to exploit the multipath diversity in frequency-selective channels. However, it is numerically shown that OCDM performs the best due to its additional time-spreading property, which is desirable for the time-dependent interference that occurs in an ANOMA system. Furthermore, for the considered scenario of two users and four blocks, we show that all the studied waveforms achieve the best performance in terms of block error rate with the derived receiver when the blocks overlap halfway.**

***Index Terms*—power-domain asynchronous NOMA, OCDM, waveform design, triangular SIC, iterative receiver**

I. Introduction

Non-orthogonal multiple access (NOMA) is a highly promising multiple access technique for the next generation of cellular communication systems. Compared to previous generations based on orthogonal multiple access (OMA), NOMA enables the reuse of the time, frequency, code, and space resources for multiple users to increase the multiuser data rate [1]. However, the improvements in the outage probability and the achievable data rate [2] come at the cost of a high receiver complexity and its vulnerability to channel estimation errors [3]. There are two main NOMA schemes: code-domain and power-domain NOMA. For code-domain NOMA, sparse or non-orthogonal cross correlation sequences with a low correlation coefficient are used for the user-specific spreading sequences [2] whereas the signals of the different users are superimposed for power-domain NOMA so that a significant power difference between the signals of the different users is present at the receiver.

Synchronous NOMA is advantageous due to a lower receiver complexity. However, it was shown in [4], [5] that a higher sum rate can be achieved if an intentional time delay between the received signals of the different users is utilized. This makes asynchronous non-orthogonal multiple access (ANOMA) with an intentional time offset attractive for high-throughput communications. In addition, the complexity of the transmitter can be reduced due to more relaxed time requirements for the uplink synchronization. At the receiver side, multiple blocks have to be processed jointly in ANOMA to cancel the interference of the other users. In order to cancel the interference pattern for uplink transmissions, triangular successive interference cancellation (T-SIC) has been proposed in [6] for power-domain ANOMA which significantly improves the bit error rate (BER) performance compared to conventional SIC. Furthermore, in [7] a message-passing signal detection scheme for equal-power transmissions is derived.

As a result of using a discrete constellation set, the input signal is not Gaussian distributed, and therefore the utilized waveform has an effect on the mutual information [8]. To maximize the mutual information assuming perfect feedback equalization, the waveform has to spread the data in a way such that the same channel gain is obtained for all symbols [8]. Considering a frequency-selective channel (FSC), an optimal waveform spreads the symbols over the whole bandwidth. In addition, another effect appears for ANOMA, i.e., the interference is not consistent over the duration of a block due to the partial overlap of the first and last blocks. To achieve an equal gain for all symbols in this case, the transmission matrix needs to spread its symbols over the whole duration of a block. Therefore, an optimal waveform for ANOMA spreads the symbols fully in the time and frequency domains like orthogonal chirp division multiplexing (OCDM) [9], [10]. A similar concept has been considered in [9], [10], where the authors have shown for cyclic prefix (CP) free transmissions that having equal levels of interference for all symbols is more advantageous than if specific symbols are more affected by the interference than others.

In the literature, the typical waveform choice for power-based ANOMA is orthogonal frequency division multiplexing (OFDM) [4]–[6]. To reduce the high peak-to-average power ratio (PAPR) of OFDM, a single-carrier (SC) based ANOMA scheme is proposed in [11] which enables the implementation of low-cost wireless terminals. In addition, SC exploits the multipath diversity which occurs in the considered FSC. However, SC does not spread its symbols in the time domain, which is sub-optimal when considering the time-localized interference presented in ANOMA. Thus, in this work, we propose OCDM for ANOMA to attain an equal gain and equal interference for all symbols.

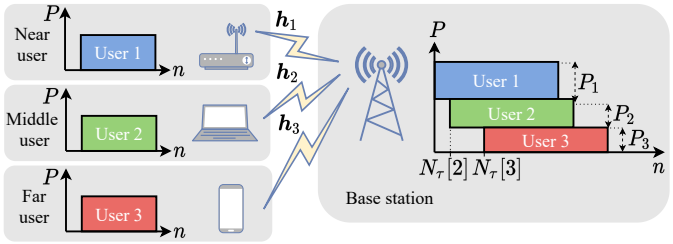

Fig. 1: Uplink ANOMA scenario.

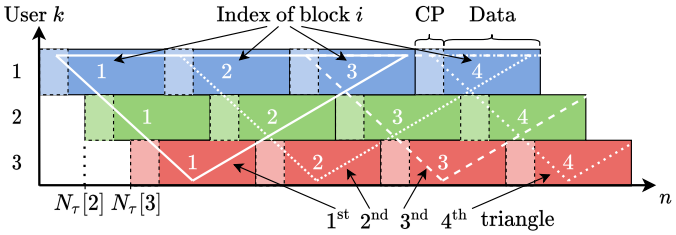

Fig. 2: Received signal in the time domain.

The main contributions of this paper are listed as follows: 1) A generic iterative receiver is derived based on soft-information T-SIC with a minimum mean square error parallel interference cancellation (MMSE-PIC) detector for uplink power-domain ANOMA. This receiver enables the use of any linear modulation for the first time. 2) OFDM, SC and OCDM are analyzed for an ANOMA scenario with two users and four blocks each. The numerical simulations show that OCDM achieves the lowest block error rate (BLER) when a significant time offset between the users is present which validates the advantage of time-frequency spreading waveforms. 3) It is shown that in the considered uplink scenario, the best BLER performance is achieved when the blocks overlap halfway.

The remainder of the paper is structured as follows: Section II presents the system model. Section III introduces the generic iterative receiver design for ANOMA. Section IV depicts the numerical results. The conclusion is given in Section V.

II. System Model

An uplink ANOMA scenario is visualized in Fig. 1 considering $K = 3$ transmitters and one base station. The signals of the K users are transmitted through the K different channels $\boldsymbol{h}_k$ and are received by the base station with the power P_k and a time offset of $N_\tau[k]$. In uplink ANOMA systems, the most important power for the receiver design is the received power P_k which is the combination of the transmission power with the channel gain. The received power ratio is given as $10\log(P_k/P_n)$ between the received power caused by the kth and nth user. The time-domain superimposed received signal is described as

$$\tilde{y}'[n] = \sum_{k=1}^{K} \sqrt{P_k} h_k[n] * x'_k[n - N_\tau[k]] + \omega'[n], \tag{1}$$

where the transmission sequence of the kth user, the channel impulse response and the additive white Gaussian noise (AWGN) are denoted as $x'_k[n]$, $h_k[n]$ and $\omega'[n]$, respectively. $N_\tau[k]$ describes the delay of the beginning of the 1st block of the kth user compared to the block which is received first. The linear convolution is marked by $*$. The channel state information (CSI) is assumed to be available at the receiver.

A. Linear Transmission Model

1) Transmitter: A number of uniformly distributed random bits $\boldsymbol{b}_{k,i} \in \{0,1\}^{N_b}$ are created for each user $k \in \{1,\dots,K\}$ and block $i \in \{1,\dots,M\}$. These bits are encoded generating the sequence $\boldsymbol{c}_{k,i} \in \{0,1\}^{N_c}$ with the code rate $r = N_c/N_b$. Given a quadrature amplitude modulation (QAM) constellation set $\mathcal{S}$ with cardinality $|\mathcal{S}| = J$, the encoded bits are mapped such that the symbol vector $\boldsymbol{d}_{k,i} \in \mathcal{S}^{N_d}$ arises and $\mathbb{E}\{\boldsymbol{d}_{k,i}\boldsymbol{d}_{k,i}^{\mathrm{H}}\} = \mathbf{I}_{N_d}$ applies. $N_d = N_c/\log_2(J)$ denotes the number of symbols. The statistical expectation, the Hermitian transpose and the identity matrix are defined as the operators $\mathbb{E}[\cdot]$, $(\cdot)^{\mathrm{H}}$ and the symbol $\mathbf{I}$. The symbol vector is modulated with the transmission matrix in the time domain $\boldsymbol{A}_{\mathrm{T}} \in \mathbb{C}^{N_d \times N_d}$ leading to the transmission samples $\boldsymbol{x}_{k,i} = \boldsymbol{A}_{\mathrm{T}}\boldsymbol{d}_{k,i}$. To simplify the equalizer notation, the modulation can be described in the frequency domain as $\boldsymbol{X}_{k,i} = \boldsymbol{A}_{\mathrm{F}}\boldsymbol{d}_{k,i}$ with the transmission frequency-domain matrix $\boldsymbol{A}_{\mathrm{F}} = \boldsymbol{F}\boldsymbol{A}_{\mathrm{T}}$. The normalized discrete Fourier transform (DFT) matrix is denoted as $\boldsymbol{F}$. Next, a CP is generated and appended to the transmission samples leading to a block. To describe the CP efficiently, the CP insertion is integrated into the matrix $\boldsymbol{A}'_{\mathrm{T}} = [[\mathbf{0}_{N_{\mathrm{CP}} \times N_d - N_{\mathrm{CP}}}; \mathbf{I}_{N_{\mathrm{CP}}}]; [\mathbf{I}_{N_d}]]\boldsymbol{A}_{\mathrm{T}}$. The coded data vector with CP can be described as $\boldsymbol{x}'_{k,i} = \boldsymbol{A}'_{\mathrm{T}}\boldsymbol{d}_{k,i}$ and has a length of $N_{x'}$. Hereafter, a CP insertion is assumed for all waveforms. The total transmission sequence of the kth user is $\boldsymbol{x}'_k = [\boldsymbol{x}'^{\mathrm{T}}_{k,0}, \boldsymbol{x}'^{\mathrm{T}}_{k,1}, \dots, \boldsymbol{x}'^{\mathrm{T}}_{k,M-1}]^{\mathrm{T}}$.

2) Waveforms: The transmission matrices of OFDM and SC are $\boldsymbol{A}_{\mathrm{T}}^{\mathrm{OFDM}} = \boldsymbol{F}^{\mathrm{H}}$ and $\boldsymbol{A}_{\mathrm{T}}^{\mathrm{SC}} = \mathbf{I}$, respectively. OFDM spreads the symbols only in the time domain and SC only in the frequency domain. For the OCDM waveform, which spreads in the time and frequency domain, the transmission matrix can be described as [8] $\boldsymbol{A}_{\mathrm{T}}^{\mathrm{OCDM}} = [\boldsymbol{g}_0, \boldsymbol{g}_1, \dots, \boldsymbol{g}_{N_d-1}]$. $\boldsymbol{g}_j$ equals the chirp for the jth symbol in $\boldsymbol{d}$ as given in [9].

B. Wireless Channel

Due to the multipath of the wireless channel, an FSC is assumed that has the impulse response $\boldsymbol{h}_k = [h_{k,0}, h_{k,1}, \dots, h_{k,L-1}]$. Here, $h_{k,l}$ is a stationary complex Gaussian process [12, p. 128] that is uncorrelated with respect to (w.r.t.) the users $k \in \{1,2,\dots,K\}$ and the channel taps $l \in \{1,2,\dots,L\}$. The discrete wireless channel is characterized by the power delay profile (PDP) and is assumed to be invariant over the whole transmission. The CP is assumed to be longer that the channel delay spread. Thus, the channel is modeled as a circular convolution given by the circulant channel matrix $\boldsymbol{H}_k$. Let $\boldsymbol{\Lambda}_k = \boldsymbol{F}\boldsymbol{H}_k\boldsymbol{F}^{\mathrm{H}}$ be a diagonal matrix whose diagonal elements correspond to the frequency-domain channel response of the kth user.

C. Received Signal

The normalized received signal can be described as

$$\tilde{\boldsymbol{y}}^{\mathrm{norm}}_{k,i} = \boldsymbol{H}_k\boldsymbol{x}_{k,i} + \boldsymbol{s}^{\mathrm{norm}}_{k,i} + \boldsymbol{w}^{\mathrm{norm}}_{k,i}, \tag{2}$$

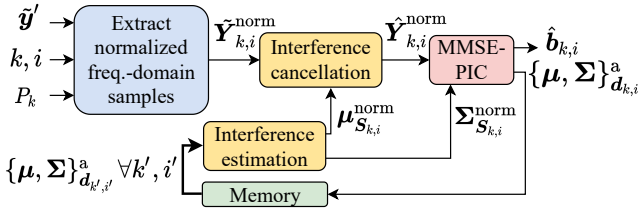

Fig. 3: Iterative receiver.

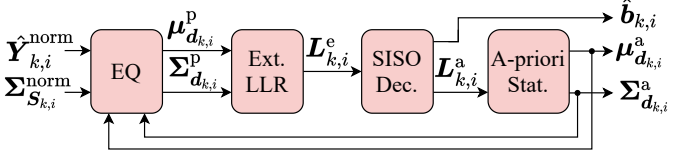

Fig. 4: MMSE-PIC detector.

with the normalized interference $\boldsymbol{s}_{k,i}^{\text{norm}} = \boldsymbol{s}_{k,i}/\sqrt{P_k}$. The normalization to the received power of the kth user is performed to obtain a similar range of values for all users within the receiver. $\boldsymbol{w}_{k,i}^{\text{norm}} \sim \mathcal{CN}(0, \sigma_k^2\mathbf{I})$ is the AWGN on the ith block of the kth user with $\sigma_k^2 = \sigma^2/P_k$. The interference of the blocks $\{i-1, i, i+1\}$ of all users except the kth user on the considered ith block of the kth user is calculated as

$$\boldsymbol{s}_{k,i} = \sum_{n=1,n\neq k}^{K} \sqrt{P_n}(\dddot{\boldsymbol{H}}_{n,k}\boldsymbol{x}'_{n,i-1} + \ddot{\boldsymbol{H}}_{n,k}\boldsymbol{x}'_{n,i} + \dot{\boldsymbol{H}}_{n,k}\boldsymbol{x}'_{n,i+1}). \quad (3)$$

The channel matrices $\dddot{\boldsymbol{H}}_{n,k}$, $\ddot{\boldsymbol{H}}_{n,k}$ and $\dot{\boldsymbol{H}}_{n,k}$ describe the influence of the $i-1$th, ith or $i+1$th block, respectively, of the nth user on the ith block of the kth user. If the interfering user has a lower index n than the user of interest k as $n < k$, then $\dddot{\boldsymbol{H}}_{n,k} = \mathbf{0}$. If the interfering user has a higher index than the user of interest as $n > k$, then $\dot{\boldsymbol{H}}_{n,k} = \mathbf{0}$. The mathematical description of the channel matrices in given in the Appendix.

III. Generic Iterative Receiver Design for ANOMA

The generic iterative receiver is shown in Fig. 3. It contains the processing blocks and the *Memory* for storing the a-priori mean and covariance of previous computations of all blocks of all users. According to the decoding schedule, the normalized frequency-domain samples of the ith block of the kth user are extracted from the received signal $\tilde{\boldsymbol{y}}'$. This requires four operations. Firstly, the relevant part $\tilde{\boldsymbol{y}}'_{k,i}$ of the received signal $\tilde{\boldsymbol{y}}'$ is extracted. Secondly, the CP is removed. Thirdly, the signal $\tilde{\boldsymbol{y}}_{k,i}$ is transformed to the frequency domain using a DFT resulting in $\tilde{\boldsymbol{Y}}_{k,i}$. Lastly, the signal is normalized according to the received power P_k leading to $\tilde{\boldsymbol{Y}}_{k,i}^{\text{norm}}$. In the following, the decoding schedule, the *Interference estimation*, the *Interference cancellation* and the *MMSE-PIC* detector are explained.

1) Decoding Schedule: Due to different receive powers of the users, the schedule in which the blocks of the users are decoded is crucial for a good overall system performance. To properly decode a block, the interfering blocks of the users with higher received power should be decoded first. This leads, in combination with the assumption that the delays N_τ of the received blocks are increasing from the user with the strongest to the lowest received power, to a triangular decoding schedule as described in [6]. The decoding triangles are visible in Fig. 2. The number of triangles corresponds to the number of blocks per user. The triangles are computed one after another starting from the one with the continuous contour. Within one triangle, the blocks are decoded starting from the user with the highest to the user with the lowest received power. If all blocks within one triangle have been computed, the decoding triangle can be reprocessed with the a-priori knowledge of the users with lower received power. The blocks within the triangle can be computed N_{TSIC} times.

2) Interference Estimation and Cancellation: The interference statistics for the ith block of the kth user are estimated by the *Interference estimation* step. The a-priori mean of the interference $\boldsymbol{\mu}_{\boldsymbol{s}_{k,i}}^{\text{a}} = \mathbb{E}\{\boldsymbol{s}_{k,i}\}$ is computed as

$$\boldsymbol{\mu}_{\boldsymbol{s}_{k,i}}^{\text{a}} = \sum_{n=1,n\neq k}^{K} \sqrt{P_n}(\dddot{\boldsymbol{H}}_{n,k}\boldsymbol{A}'_{\text{T}}\boldsymbol{\mu}_{\boldsymbol{d}_{n,i-1}}^{\text{a}} + \ddot{\boldsymbol{H}}_{n,k}\boldsymbol{A}'_{\text{T}}\boldsymbol{\mu}_{\boldsymbol{d}_{n,i}}^{\text{a}} + \dot{\boldsymbol{H}}_{n,k}\boldsymbol{A}'_{\text{T}}\boldsymbol{\mu}_{\boldsymbol{d}_{n,i+1}}^{\text{a}}), \quad (4)$$

and the a-priori covariance of the interference as

$$\begin{aligned}\boldsymbol{\Sigma}_{\boldsymbol{s}_{k,i}}^{\text{a}} &= \mathbb{E}\{(\boldsymbol{s}_{k,i} - \boldsymbol{\mu}_{\boldsymbol{s}_{k,i}}^{\text{a}})(\boldsymbol{s}_{k,i} - \boldsymbol{\mu}_{\boldsymbol{s}_{k,i}}^{\text{a}})^{\text{H}}\} \quad (5)\\ &= \sum_{n=1,n\neq k}^{K} P_n(\dddot{\boldsymbol{H}}_{n,k}\boldsymbol{A}'_{\text{T}}\boldsymbol{\Sigma}_{\boldsymbol{d}_{n,i-1}}^{\text{a}}\boldsymbol{A}'^{\text{H}}_{\text{T}}\dddot{\boldsymbol{H}}^{\text{H}}_{n,k} + \ddot{\boldsymbol{H}}_{n,k}\boldsymbol{A}'_{\text{T}}\boldsymbol{\Sigma}_{\boldsymbol{d}_{n,i}}^{\text{a}}\boldsymbol{A}'^{\text{H}}_{\text{T}}\ddot{\boldsymbol{H}}^{\text{H}}_{n,k} + \dot{\boldsymbol{H}}_{n,k}\boldsymbol{A}'_{\text{T}}\boldsymbol{\Sigma}_{\boldsymbol{d}_{n,i+1}}^{\text{a}}\boldsymbol{A}'^{\text{H}}_{\text{T}}\dot{\boldsymbol{H}}^{\text{H}}_{n,k}).\end{aligned}$$

Here, the a-priori covariance matrix of the symbols $\boldsymbol{d}_{n,i}$ is given as $\boldsymbol{\Sigma}_{\boldsymbol{d}_{n,i}}^{\text{a}} = \mathbb{E}\{(\boldsymbol{d}_{n,i} - \boldsymbol{\mu}_{\boldsymbol{d}_{n,i}}^{\text{a}})(\boldsymbol{d}_{n,i} - \boldsymbol{\mu}_{\boldsymbol{d}_{n,i}}^{\text{a}})^{\text{H}}\}$. The a-priori mean $\boldsymbol{\mu}_{\boldsymbol{d}_{n,i}}^{\text{a}}$ and a-priori covariance matrix $\boldsymbol{\Sigma}_{\boldsymbol{d}_{n,i}}^{\text{a}}$ are provided by the *A-priori Stat.* step that is explained in Section III-3b. If no a-priori knowledge is available about the interfering block, the a-priori mean is assumed to be zero $\boldsymbol{\mu}_{\boldsymbol{d}_{n,i}}^{\text{a}} = \mathbf{0}$. The cross terms in (5) are zero due to the uncorrelated symbols of the transmission blocks. Thus, the covariances of the interfering users can be added. Both the a-priori mean and covariance of the interference are transformed to the frequency domain for the use in the equalizer as $\boldsymbol{\mu}_{\boldsymbol{S}_{k,i}}^{\text{a}} = \boldsymbol{F}\boldsymbol{\mu}_{\boldsymbol{s}_{k,i}}^{\text{a}}$ and $\boldsymbol{\Sigma}_{\boldsymbol{S}_{k,i}}^{\text{a}} = \boldsymbol{F}\boldsymbol{\Sigma}_{\boldsymbol{s}_{k,i}}^{\text{a}}\boldsymbol{F}^{\text{H}}$, respectively. Moreover, the estimates are normalized to the kth transmission power P_k as $\boldsymbol{\mu}_{\boldsymbol{S}_{k,i}}^{\text{norm}} = \boldsymbol{\mu}_{\boldsymbol{S}_{k,i}}^{\text{a}}/\sqrt{P_k}$ and $\boldsymbol{\Sigma}_{\boldsymbol{S}_{k,i}}^{\text{norm}} = \boldsymbol{\Sigma}_{\boldsymbol{S}_{k,i}}^{\text{a}}/P_k$, respectively. Based on the a-priori mean of the interference, the *Interference cancellation* is executed as

$$\hat{\boldsymbol{Y}}_{k,i}^{\text{norm}} = \tilde{\boldsymbol{Y}}_{k,i}^{\text{norm}} - \boldsymbol{\mu}_{\boldsymbol{S}_{k,i}}^{\text{norm}}. \quad (6)$$

3) MMSE-PIC Detector: The MMSE-PIC detector for ANOMA is derived based on the synchronous OMA implementation of [10] and is depicted in Fig. 4. The MMSE-PIC detector computes the a-priori mean and the covariance of the symbols of the ith block of the kth user $\boldsymbol{\mu}_{\boldsymbol{d}_{k,i}}^{\text{a}}$ and $\boldsymbol{\Sigma}_{\boldsymbol{d}_{k,i}}^{\text{a}}$, respectively, and calculates the estimated bits $\hat{\boldsymbol{b}}_{k,i}$ from the normalized interference-cancelled signal in the frequency domain $\hat{\boldsymbol{Y}}_k^{\text{norm}}$ and the a-priori interference covariance matrix $\boldsymbol{\Sigma}_{\boldsymbol{S}_k}^{\text{norm}}$. N_{Eq} iterations of the MMSE-PIC are computed. However, the execution can be stopped if the correct bits are detected by the cyclic redundancy check (CRC).

a) Equalizer: Assuming an OMA system, the component-wise conditionally unbiased (CWCU) linear minimum mean square error (LMMSE) equalization is described in [10]. However, for ANOMA the considered ith block of the kth user should be specified and the interference $\boldsymbol{S}_{k,i}$ should be considered. With the a-priori estimates of the interference, the a-posteriori mean of the symbol vector can be computed by the CWCU LMMSE equalizer as

$$\boldsymbol{\mu}^{\mathrm{p}}_{\boldsymbol{d}_{k,i}} = \boldsymbol{\mu}^{\mathrm{a}}_{\boldsymbol{d}_{k,i}} + \bar{\boldsymbol{\Gamma}}^{-1}_{k,i} \boldsymbol{A}_{\mathrm{F}}^{\mathrm{H}} \boldsymbol{\Lambda}_k^{\mathrm{H}} \boldsymbol{\Sigma}^{\mathrm{norm}}_{\boldsymbol{Y}_{k,i}} (\hat{\boldsymbol{Y}}^{\mathrm{norm}}_{k,i} - \boldsymbol{\Lambda}_k \boldsymbol{A}_{\mathrm{F}} \boldsymbol{\mu}^{\mathrm{a}}_{\boldsymbol{d}_{k,i}}), \quad (7)$$

with the a-posteriori covariance matrix

$$\boldsymbol{\Sigma}^{\mathrm{p}}_{\boldsymbol{d}_{k,i}} = \bar{\boldsymbol{\Gamma}}^{-1}_{k,i} - \boldsymbol{\Sigma}^{\mathrm{a}}_{\boldsymbol{d}_{k,i}}. \quad (8)$$

The CWCU normalization is performed through the multiplication of the inverse of the diagonal matrix $\bar{\boldsymbol{\Gamma}} = \mathrm{diag}\{\boldsymbol{\Gamma}_{1,1}, \boldsymbol{\Gamma}_{2,2}, \ldots, \boldsymbol{\Gamma}_{N_d,N_d}\}$ where the matrix $\boldsymbol{\Gamma}_{k,i}$ is defined as $\boldsymbol{\Gamma}_{k,i} = \boldsymbol{A}_{\mathrm{F}}^{\mathrm{H}} \boldsymbol{\Lambda}_k^{\mathrm{H}} \boldsymbol{\Sigma}^{\mathrm{norm}}_{\boldsymbol{Y}_{k,i}} \boldsymbol{\Lambda}_k \boldsymbol{A}_{\mathrm{F}}$. This operation leads to unitary diagonal elements of the equalization matrix and thus, assures CWCU estimates of $\boldsymbol{\mu}^{\mathrm{p}}_{\boldsymbol{d}_{k,i}}$. After the interference cancellation, the covariance matrix of the received signal is estimated as

$$\boldsymbol{\Sigma}^{\mathrm{norm}}_{\boldsymbol{Y}_{k,i}} = (\boldsymbol{\Lambda}_k \boldsymbol{A}_{\mathrm{F}} \boldsymbol{\Sigma}^{\mathrm{a}}_{\boldsymbol{d}_{k,i}} \boldsymbol{A}_{\mathrm{F}}^{\mathrm{H}} \boldsymbol{\Lambda}_k^{\mathrm{H}} + \boldsymbol{\Sigma}^{\mathrm{norm}}_{\boldsymbol{S}_{k,i}} + \sigma_k^2 \mathbf{I})^{-1}. \quad (9)$$

b) Extrinsic LLR, SISO Decoder and A-priori Statistics: The extrinsic log-likelihood ratio (LLR) $\boldsymbol{L}^{e}_{k,i}$ is calculated in the *Extrinsic LLR* block, the a-priori LLRs of the coded bits $\boldsymbol{L}^{\mathrm{a}}_{k,i}$ and the estimated information bits $\hat{\boldsymbol{b}}_{k,i}$ in the *SISO decoder* and the the a-priori mean $\boldsymbol{\mu}^{\mathrm{a}}_{\boldsymbol{d}_{k,i}}$ and the covariance $\boldsymbol{\Sigma}^{\mathrm{a}}_{\boldsymbol{d}_{k,i}}$ in the *A-priori Stat.* block as described in [13]. The MMSE-PIC detector calculates in every iteration the a-priori mean estimate $\boldsymbol{\mu}^{\mathrm{a}}_{\boldsymbol{d}_{k,i}}$ and the covariance estimate $\boldsymbol{\Sigma}^{\mathrm{a}}_{\boldsymbol{d}_{k,i}}$. However, the a-priori estimates that are generated in the first iteration of the detector are forwarded to the *Memory* if the considered block was not decoded correctly after N_{Eq} iterations. It was shown in [13] that this is reasonable because the MMSE-PIC detector can converge to incorrect values which would deteriorate the interference cancellation performance. If the CRC detects that an interfering block was decoded successfully, $\boldsymbol{\mu}^{\mathrm{a}}_{\boldsymbol{d}_{k,i}} = \boldsymbol{d}_{k,i}$ is valid and will be stored. Subsequently, the whole interference of this block on the other blocks can be subtracted.

IV. Numerical Evaluation and Discussion

The BLER of the derived ANOMA receiver is numerically analyzed for two users based on the parameters given in Tab. I and the extended vehicular A (EVA) channel model in [14]. The impact of the delay between the users and their power ratio $10\log(P_1/P_2)$ are investigated for different waveforms.

A. Impact of the Delay

The delay between the different users is critical in ANOMA. Therefore, the question arises how the delay impacts the system performance. A simulation is conducted where the power ratio is fixed to 5 dB and the received SNR of the 1st user to 15 dB. The normalized delay $\tau = N_\tau / N_{x'}$ is variable, ranging from $\tau = 0$ (perfect overlap of block i of the 1st user with block i of the 2nd user) to $\tau = 1$ (perfect overlap of block $i+1$ of the 1st user with block i of the 2nd user). The BLER is shown in Fig. 5. It can be noticed that between $0.1 < \tau < 0.9$ OCDM performs better than SC for the 1st user which can be explained by the time spreading advantage for the time-localized interference in ANOMA. For the 2nd user no significant difference is evident. OFDM has a worse performance compared to the other waveforms due to no frequency spreading. An increased delay leads to a smaller overlap between the 1st blocks of both users, so the BLER for the 1st block of the 1st user decreases due to less interference. Through the T-SIC, the interference cancellation (IC) of all blocks are interconnected. Thus, the improvement of the 1st block of the 1st user affects all other blocks leading to a lower BLER overall. For a more detailed explanation about the T-SIC concept, refer to [6]. The increase of τ beyond 0.5 however, decreases the overall performance. In this case, the IC is less effective for the 1st block of the 2nd user, because this block has a larger overlap with the 2nd block of the 1st user rather than the 1st block. This is unfavorable because the 2nd block of the 1st user has more interference and therefore a less reliable estimation for the IC. This explains the U-shape with the best performance at a medium delay between $0.4 \leq \tau \leq 0.6$. That $\tau = 0.5$ is the optimal normalized timing mismatch to maximize the sum throughput in a two-user ANOMA system was shown in [4] for an infinite number of symbols in a frame. In this simulation, only a finite amount of $M = 4$ blocks is simulated but it can be seen that the T-SIC propagation with the normalized delay $\tau = 0.5$ reaches the best BLER performance in this scenario. However, the sum throughput $(1 - \mathrm{BLER})/((M + \tau)N_{x'})$ is dependent on the delay τ. If this is considered, the delay for the optimal throughput lies between $0 \leq \tau \leq 0.5$. However the optimal throughput is not investigated in this work. Furthermore, in future work, the T-SIC scheme for a delay $\tau \geq 0.5$ can be adjusted to benefit from the low interference of the last block of the 2nd user.

TABLE I: Simulation settings.

Parameter	Value
Bandwidth	$B = 4.32$ MHz
Channel delay spread	$L = 12$ samples
Normalized delay	$0 \leq \tau \leq 1$
Number of users and blocks	$K = 2$ users, $M = 4$ blocks
Number of samples per block	$N_d = 128$ samples
Length of CP	$N_{\mathrm{CP}} = 16$ samples
Modulation and coding	4-QAM with 1/2 code rate
Encoder	Recursive Systematic Conv. with $[1\ 13/15]_8$
Decoder	BCJR log-MAP
Iterations T-SIC and equalizer	$N_{\mathrm{TSIC}} = 2$ iterations, $N_{\mathrm{Eq}} = 7$ iterations

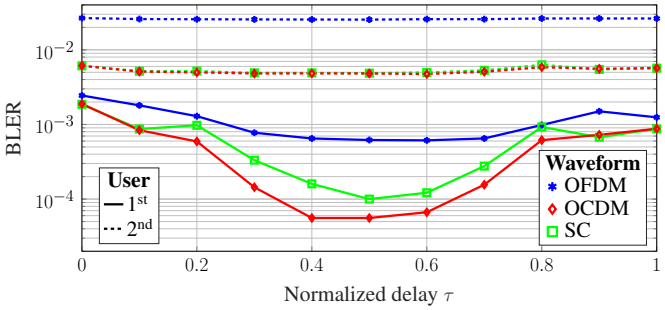

Fig. 5: BLER dependent on the normalized delay τ.

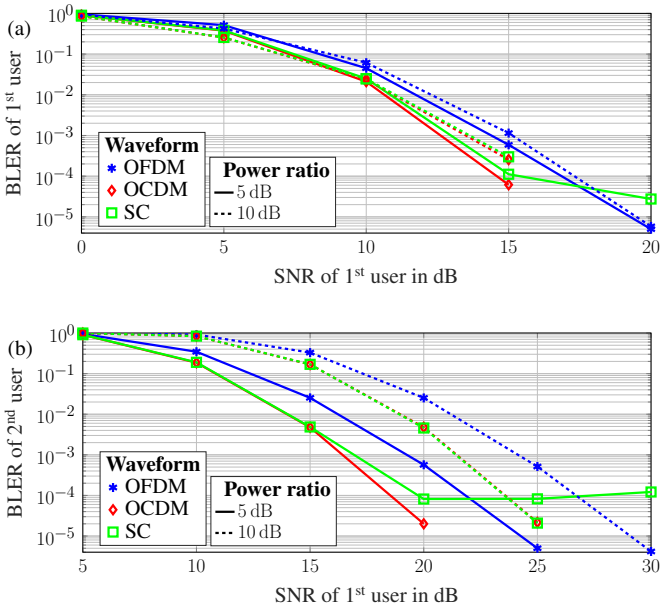

Fig. 6: BLER for different power ratios for $\tau = 0.5$.

B. Impact of the Power Ratio

The BLER of the 1st and the 2nd user for a fixed delay in dependence on the power ratio are shown in Fig. 6a and Fig. 6b, respectively. $\tau = 0.5$, which has been shown to be optimal for the considered scenario in Fig. 5. For both users, the performance differs considerably between SC, OCDM and OFDM. For the high power ratio of $10\,\mathrm{dB}$, OCDM and SC have a similar BLER but significantly lower than OFDM. This is due to the frequency spreading of OCDM and SC which is an advantage compared to OFDM. For the low power ratio of $5\,\mathrm{dB}$, OCDM and SC perform alike, however, at high SNR $>$ $15\,\mathrm{dB}$ OCDM has a lower BLER. This can be explained with the time-speading property of OCDM which helps to attain an equal gain for the symbols even at low SNR. An error floor is visible for SC at the low power ratio of $5\,\mathrm{dB}$. The error floor for SC is analyzed for NOMA in our previous work [13] and results from convergence effect in the MMSE-PIC detector if blocks are decoded incorrectly. The simulations show that this effect is lower for OCDM since there is no visible error floor, which make OCDM an excellent waveform for ANOMA.

V. Conclusion

In this paper, a generic iterative receiver is derived for ANOMA which enables the use of any linearly modulated waveform. For this, T-SIC is implemented based on soft-information and is combined with an MMSE-PIC detector. Regarding the waveforms, OFDM, SC and OCDM are investigated. It is numerically shown that OCDM outperforms SC and OFDM for ANOMA. This is due to its time-spreading property which leads to an equal symbol gain despite of the time-dependent interference that occurs in ANOMA system combined with its frequency-spreading property which is desirable for the considered FSC. Furthermore, this work has shown that for the analyzed scenario the best BLER performance for any waveform is achieved if the blocks overlap halfway.

Appendix

The matrices $\ddot{\boldsymbol{H}}_{n,k}$, $\ddot{\boldsymbol{H}}_{n,k}$ and $\dot{\boldsymbol{H}}_{n,k}$ can be described with the help of the extended channel matrix

$$\boldsymbol{H}_n^* = [\boldsymbol{0}_{N_d \times N_{x'}},\ \boldsymbol{H}_n',\ \boldsymbol{0}_{N_d \times N_{x'}}] \in \mathbb{C}^{N_d \times 3N_{x'}}, \tag{10}$$

and the shift matrix $\boldsymbol{L}_\tau \in \mathbb{N}^{3N_{x'} \times 3N_{x'}}$. $\boldsymbol{H}_n' \in \mathbb{C}^{N_d \times N_{x'}}$ describes the channel matrix considering the CP insertion. $L_{\tau[n,k]}[i,j] = \delta_{i,j-N_\tau[n,k]}$ describes the shift matrix with the Kronecker delta symbol of the $[i,j]$-th component $\delta_{i,j}$. The delay $N_\tau[n,k] = N_\tau[k] - N_\tau[n]$ is dependent on the user k which is interfered by user n. The channel interference matrices can be computed through the multiplication of the extended channel matrix with the shift matrix as

$$[\ddot{\boldsymbol{H}}_{n,k}, \ddot{\boldsymbol{H}}_{n,k}, \dot{\boldsymbol{H}}_{n,k}] = \boldsymbol{H}_n^* \boldsymbol{L}_{\tau[n,k]}. \tag{11}$$

The received frequency-domain signal and interference can be calculated as $\tilde{\boldsymbol{Y}}_{k,i} = \boldsymbol{F}\tilde{\boldsymbol{y}}_{k,i}$ and $\boldsymbol{S}_{k,i} = \boldsymbol{F}\boldsymbol{s}_{k,i}$, respectively.

Acknowledgment

This project has received funding from the EU's Horizon 2020 research and innovation programme through the project iNGENIOUS under grant agreement No. 957216.

References

[1] L. Dai, B. Wang, Z. Ding, Z. Wang, S. Chen, and L. Hanzo, "A Survey of Non-Orthogonal Multiple Access for 5G," *IEEE Commun. Surveys Tuts.*, vol. 20, no. 3, pp. 2294–2323, 2018.

[2] S. M. R. Islam, N. Avazov, O. A. Dobre, and K. Kwak, "Power-Domain Non-Orthogonal Multiple Access (NOMA) in 5G Systems: Potentials and Challenges," *IEEE Commun. Surveys Tuts.*, vol. 19, no. 2, pp. 721–742, 2017.

[3] M. M. Şahin and H. Arslan, "Waveform-Domain NOMA: The Future of Multiple Access," in *2020 IEEE Int. Conf. on Commun. Workshops*, 2020, pp. 1–6.

[4] X. Zou, B. He, and H. Jafarkhani, "An Analysis of Two-User Uplink Asynchronous Non-orthogonal Multiple Access Systems," *IEEE Trans. Wireless Commun.*, vol. 18, no. 2, pp. 1404–1418, 2019.

[5] C. Liu and N. C. Beaulieu, "Exact BER Performance for Symbol-Asynchronous Two-User Non-Orthogonal Multiple Access," *IEEE Commun. Lett.*, vol. 25, no. 3, pp. 764–768, 2021.

[6] H. Haci, H. Zhu, and J. Wang, "Performance of non-orthogonal multiple access with a novel asynchronous interference cancellation technique," *IEEE Trans. Commun*, vol. 65, no. 3, pp. 1319–1335, 2017.

[7] J. Liu, Y. Li, G. Song, and Y. Sun, "Detection and Analysis of Symbol-Asynchronous Uplink NOMA With Equal Transmission Power," *IEEE Wireless Commun. Lett.*, vol. 8, no. 4, pp. 1069–1072, 2019.

[8] R. Bomfin, D. Zhang, M. Matthé, and G. Fettweis, "A Theoretical Framework for Optimizing Multicarrier Systems Under Time and/or Frequency-Selective Channels," *IEEE Commun. Lett.*, vol. 22, no. 11, pp. 2394–2397, 2018.

[9] X. Ouyang and J. Zhao, "Orthogonal chirp division multiplexing," *IEEE Trans. Commun.*, vol. 64, no. 9, pp. 3946–3957, 2016.

[10] R. Bomfin, M. Chafii, and G. Fettweis, "Low-Complexity Iterative Receiver for Orthogonal Chirp Division Multiplexing," in *2019 IEEE Wireless Commun. and Netw. Conf. Workshop*, 2019, pp. 1–6.

[11] H. Liu, T. A. Tsiftsis, K. J. Kim, K. S. Kwak, and H. V. Poor, "Rate Splitting for Asynchronous Uplink NOMA Systems with Cyclic Prefixed Single Carrier," in *2019 IEEE Int. Conf. on Commun. Workshops*, 2019, pp. 1–6.

[12] A. Molisch, *Wireless Communications*. Wiley-IEEE Press, 2011.

[13] M. Sigmund, R. Bomfin, M. Chafii, A. Nimr, and G. Fettweis, "Iterative Receiver for Power-Domain NOMA with Mixed Waveforms," in *2022 IEEE Wireless Commun. and Netw. Conf.*, 2022.

[14] 3GPP, "LTE; Evolved Universal Terrestrial Radio Access (E-UTRA); Base Station (BS) conformance testing," 3rd Generation Partnership Project (3GPP), Technical Specification (TS) 36.141, 10 2010, v8.4.0.